4-Hydroxyacetophenone monooxygenase from Pseudomonas fluorescens ACB - A novel flavoprotein catalyzing Baeyer-Villiger oxidation of aromatic compounds

Kamerbeek, Nanne M.; Moonen, Mariëlle J.H.; Ven, Jos G.M. van der; Berkel, Willem J.H. van; Fraaije, Marco W.; Janssen, Dick B.

Published in:
European Journal of Biochemistry

DOI:
10.1046/j.1432-1327.2001.02137.x

Publication date:
2001

Eur. J. Biochem. **268**, 2547–2557 (2001) © FEBS 2001

4-Hydroxyacetophenone monooxygenase from *Pseudomonas fluorescens* ACB

A novel flavoprotein catalyzing Baeyer–Villiger oxidation of aromatic compounds

Nanne M. Kamerbeek[1], Mariëlle J. H. Moonen[2], Jos G. M. van der Ven[1,*], Willem J. H. van Berkel[2], Marco W. Fraaije[1] and Dick B. Janssen[1]

[1]*Laboratory of Biochemistry, Groningen Biomolecular Sciences and Biotechnology Institute, University of Groningen, the Netherlands;* [2]*Laboratory of Biochemistry, Department of Agrotechnology and Food Sciences, Wageningen University, the Netherlands*

A novel flavoprotein that catalyses the NADPH-dependent oxidation of 4-hydroxyacetophenone to 4-hydroxyphenyl acetate, was purified to homogeneity from *Pseudomonas fluorescens* ACB. Characterization of the purified enzyme showed that 4-hydroxyacetophenone monooxygenase (HAPMO) is a homodimer of ≈ 140 kDa with each subunit containing a noncovalently bound FAD molecule. HAPMO displays a tight coupling between NADPH oxidation and substrate oxygenation. Besides 4-hydroxyacetophenone a wide range of other acetophenones are readily converted via a Baeyer–Villiger rearrangement reaction into the corresponding phenyl acetates. The *P. fluorescens* HAPMO gene (*hapE*) was characterized. It encoded a 640 amino-acid protein with a deduced mass of 71 884 Da. Except for an N-terminal extension of ≈ 135 residues, the sequence of HAPMO shares significant similarity with two known types of Baeyer–Villiger monooxygenases: cyclohexanone monooxygenase (27–33% sequence identity) and steroid monooxygenase (33% sequence identity). The HAPMO sequence contains several sequence motifs indicative for the presence of two Rossman fold domains involved in FAD and NADPH binding. The functional role of a recently identified flavoprotein sequence motif (ATG) was explored by site-directed mutagenesis. Replacement of the strictly conserved glycine (G490) resulted in a dramatic effect on catalysis. From a kinetic analysis of the G490A mutant it is concluded that the observed sequence motif serves a structural function which is of importance for NADPH binding.

Keywords: aromatic ketones; Baeyer–Villiger monooxygenase; flavoprotein; 4-hydroxyacetophenone monooxygenase; mutagenesis.

The aerobic degradation of aromatic compounds by soil bacteria depends on the activity of oxygenases [1]. So far two classes of flavoprotein hydroxylases have been shown to act as aromatic monooxygenases: the single component aromatic hydroxylases [2] and two-component hydroxylases [3,4]. The single component aromatic hydroxylases share a typical dinucleotide binding fold for complexation of the FAD cofactor while lacking a NAD(P) binding fold [5]. An extensively studied member of this widespread class of flavoenzymes is *p*-hydroxybenzoate hydroxylase [6,7]. Mechanistic studies have shown that the monooxygenation reactions catalysed by single component aromatic hydroxylases are preceded by NAD(P)H-mediated flavin reduction. The reduced flavin then reacts with dioxygen to form a reactive electrophilic hydroperoxyflavin intermediate which is able to introduce a hydroxyl group into an activated aromatic ring [8]. The two-component hydroxylases typically consist of a relatively small flavin reductase which generates reduced flavin at the expense of NAD(P)H. After intermolecular transfer, the reduced flavin is used by the large oxygenating component to catalyse substrate hydroxylation [9,10]. Although the genes of several of these two-component hydroxylases have been identified, mechanistic data on this type of monooxygenases are scarce.

Except for the above-mentioned monooxygenation reactions another route of flavoenzyme-mediated oxygenation of aromatic compounds has been suggested in the literature. For several bacteria it was found that their ability to degrade aromatic compounds depends on an enzyme-mediated Baeyer–Villiger reaction in which an oxygen atom is inserted between the aromatic ring and a ketone side chain (Scheme 1). These Baeyer–Villiger reactions have been detected during studies on the microbial degradation of several ring-substituted acetophenones [11–13] and 4-ethylphenol [14,15]. Recently, a Baeyer–Villiger monooxygenase from *Pseudomonas putida* JD1, involved

Correspondence to D. B. Janssen, Laboratory of Biochemistry, Department of Chemistry, University of Groningen, Nijenborgh 4, 9747 AG Groningen, the Netherlands. Fax: +31 503634165, Tel.: +31 503634209, E-mail: d.b.janssen@chem.rug.nl

Abbreviations: DIG, digoxigenin; HAPMO, 4-hydroxyacetophenone monooxygenase.

Enzymes: catalase (EC. 1.11.1.6); cyclohexanone monooxygenase (EC. 1.14.13.22); 4-hydroxyacetophenone monooxygenase (EC. 1.14.13.x); 4-hydroxyphenyl acetate hydrolase (EC. 3.1.1.x); steroid monooxygenase (EC. 1.14.13.54).

**Present address*: Diosynth B.V., Akzo Nobel, Apeldoorn, the Netherlands.

Note: a web site is available at URL: www.chem.rug.nl/biotechnology

Note: The novel nucleotide sequence data published here have been submitted to Genbank and are available under accession number AF355751.

(Received 22 December 2000, revised 14 February 2001, accepted 5 March 2001)

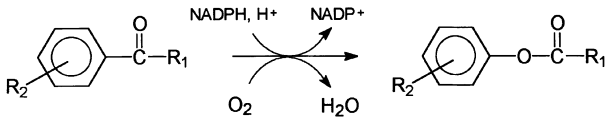

Scheme 1.

in 4-ethylphenol metabolism, was purified and partially characterized [16]. However, enzymes involved in these atypical metabolic pathways have never been cloned.

All Baeyer–Villiger monooxygenases identified so far were shown to be flavoproteins [17]. As for the single component hydroxylases, also for these enzymes a peroxygenated flavin has been proposed as the oxygenating species [18]. However, in the Baeyer–Villiger reaction this reactive flavin intermediate is supposed to act as a nucleophile indicating that in these monooxygenases a peroxyflavin anion is involved in substrate attack [19,20].

Pseudomonas fluorescens ACB is able to use 4-hydroxyacetophenone as sole carbon and energy source [13]. Since it was suggested that the microbial degradation of this phenolic compound is initiated by a Baeyer–Villiger reaction (Scheme 1), we started a study to identify this atypical aromatic monooxygenase. We report here on the purification, gene cloning, sequence analysis and characterization of 4-hydroxyacetophenone monooxygenase (HAPMO). It is shown that the enzyme is a FAD-dependent Baeyer–Villiger monooxygenase that is active with a wide range of aromatic ketones. A preliminary report on the purification of HAPMO from *P. fluorescens* ACB has been presented elsewhere [21].

MATERIALS AND METHODS

Chemicals

Restriction enzymes, 7-deaza-dGTP, and isopropyl thio-β-D-galactoside were obtained from Roche. NADH, NADPH, dithiothreitol, glucose oxidase (grade II) and catalase were from Boehringer. Tris, FAD, FMN and riboflavin were from Sigma. Q-Sepharose Fast Flow, phenyl-Sepharose Fast Flow, Superdex 200 Prep Grade, Superdex PG200 HR 10/30 and molecular weight markers were from Pharmacia. Bio-Gel P-6DG and Macro-Prep Ceramic Hydroxyapatite (Type I, particle size 20 μm) were from Bio-Rad. Acrylamide, bisacrylamide and Coomassie brilliant blue G250 were from Serva. Aromatic ketones were purchased from Acros, Aldrich, Fluorochem and Lancaster. Stock ketone solutions were prepared in dimethyl formamide. $H_2^{18}O$ (97 atom % ^{18}O) was from Campro (Elst, the Netherlands). All other chemicals were of commercially available analytical grade.

Bacterial strains and culture conditions

P. fluorescens ACB was kindly provided by D. D. Focht (University of California, Riverside, USA). *P. fluorescens* ACB was isolated from activated sewage sludge by enrichment and serial transfer with 4-hydroxyacetophenone as growth substrate [13] and grown in 0.8% Nutrient Broth (Difco) at 30 °C or in minimal medium based on Kröckel and Focht [22], containing per litre demineralized water: 3.5 g Na_2HPO_4, 1.4 g KH_2PO_4, 0.5 g $(NH_4)_2SO_4$, 0.2 g $MgSO_4.7H_2O$, 10 mg yeast extract and 5 mL of a trace elements solution. The trace elements solution contained per litre: 780 mg $Ca(NO_3)_2{\cdot}4H_2O$, 200 mg $FeSO_4{\cdot}7H_2O$, 10 mg $ZnSO_4{\cdot}7H_2O$, 10 mg H_3BO_3, 11.8 mg $CoSO_4{\cdot}7H_2O$, 4 mg $MnSO_4{\cdot}1H_2O$, 3 mg $Na_2MoO_4{\cdot}2H_2O$, 2 mg $NiCl_2{\cdot}6H_2O$, 10 mg $CuSO_4{\cdot}5H_2O$ and 2 mg $Na_2WO_4{\cdot}2H_2O$ (adjusted to pH 2 with H_2SO_4). The final pH of the medium was 7.0. Cells were grown on 10 mM 4-hydroxyacetophenone at 30 °C in 2 L Erlenmeyer flasks agitated at 270 r.p.m. on an orbital shaker to provide suitable aeration. Large-scale growth, with 4-hydroxyacetophenone as the sole carbon and energy source, was performed batchwise in a 200-L fermentor (Bioengineering AG) at 30 °C. During growth, the medium was stirred at 150 r.p.m. and flushed with 30 L air·min^{-1} and the pH was kept constant at pH 7.0 with NaOH. The fermentor was inoculated with 2 L cell culture, and growth was induced by the addition of 5 mM 4-hydroxyacetophenone, followed by two portions of 10 mM 4-hydroxyacetophenone at 8-h intervals. The cells were harvested after 24 h and the cell paste (≈ 235 g wet weight) was frozen and stored at −80 °C. Under these conditions, no significant loss of HAPMO activity occurred over a period of 6 months.

Escherichia coli strains HB101, TOP10F′ and BL21(DE3) pLysS were grown in Luria–Bertani medium supplemented with the appropriate antibiotic at 20, 30 or 37 °C.

Enzyme purification from *P. fluorescens* ACB

HAPMO was purified from *P. fluorescens* ACB to apparent homogeneity in two chromatographic steps. All purification steps were performed at 4 °C. Cells (200 g wet weight) were suspended in 21 mM potassium phosphate pH 7.1, and disrupted through a precooled Manton Gaulin press. The clarified cell extract was treated with 0.25% (w/v) protamine sulfate and the supernatant obtained after centrifugation was loaded onto a Q-Sepharose column (5 × 25 cm), equilibrated in 21 mM potassium phosphate pH 7.1. After washing with 2 vol. starting buffer, the HAPMO activity was eluted with a linear gradient of 0–0.7 M KCl in starting buffer. Active fractions were concentrated by ultrafiltration (Amicon YM-30 membrane) and diluted with 3 vol. 10 mM potassium phosphate, pH 7.1. The enzyme solution was then adjusted to 1 M ammonium sulfate and loaded onto a phenyl Sepharose column (2.5 × 40 cm), equilibrated in 50 mM potassium phosphate pH 7.1, containing 1 M ammonium sulfate. After washing with starting buffer, the HAPMO activity was eluted with a linear descending gradient of 1–0 M ammonium sulfate in 50 mM potassium phosphate, pH 7.1. Active fractions were concentrated by ultrafiltration, dialysed in 50 mM potassium phosphate, pH 7.1, and stored at −80 °C.

The 4-hydroxyphenyl acetate hydrolase was purified from *P. fluorescens* ACB in three chromatographic steps. Cell extract was loaded on a DEAE–Sepharose column (6 × 2.5 cm) equilibrated in 21 mM phosphate pH 7.1. Esterase activity was eluted with a linear gradient of 0–0.7 M KCl in starting buffer. Active fractions were pooled, dialysed against 1 mM phosphate pH 7.1, and loaded on a hydroxyapatite column (7 × 3 cm) equilibrated in 1 mM phosphate pH 7.1. Esterase activity was eluted with a linear gradient of 1–100 mM phosphate

pH 7.1. Active fractions were pooled, concentrated and loaded on a Sephacryl S-200 column (34 × 1 cm) running in 21 mM potassium phosphate, pH 7.1. The fractions with the highest esterase activity were pooled, resulting in an enzyme preparation which was more than 75% pure. For N-terminal sequencing, the esterase was isolated from a SDS-containing polyacrylamide gel.

Preparation of the genomic library

All DNA isolation and cloning procedures were carried out essentially as described by Sambrook *et al*. [23]. A genomic library of *P. fluorescens* ACB was constructed in the cosmid vector pLAFR3 according to the strategy described by Staskawicz *et al*. [24]. CsCl gradient centrifugation was used to purify pLAFR3 isolated from *E. coli* HB101. Constructed vector arms and inserts were ligated and subsequently packaged *in vitro* with a DNA-packaging kit (Boehringer). *E. coli* HB101 cells were infected with the packaging mix and transducts were selected on Luria–Bertani plates supplemented with tetracycline. From 10 transducts the plasmids were isolated and checked for insert by restriction analysis. All contained insert with an estimated average size of 17 kb. A total number of 2400 colonies was transferred to 96-well microtiter plates containing Luria–Bertani and tetracycline. After overnight growth, glycerol was added and the library was stored at −80 °C until use.

'Touch down' PCR on total DNA

All PCR amplifications were performed as described by Innis and Gelfand [25]. The 50-μL reaction mixtures contained PCR buffer (Roche), 200 μM of each dNTP, 20–30 pmol primer, 1–5 units *Taq* or *Pwo* polymerase and 10–100 ng template.

The following degenerated primers were designed on the N-terminal amino-acid sequences of the purified enzymes: HAPMO, PAMOACB1 (forward) 5′-GAAACCATGGCN GCNTTYAAYACNACNYTNCC-3′ and PAMOACB2 (reverse) 5′-GAAAACCATGGRTCRTCRTCRTARTCNA RNGWNGG-3′; esterase (4-hydroxyphenyl acetate hydrolase), PESACB1 (forward) 5′-GAAACCATGGCNCTNG AYGTNGARWCNGCNCARCTNCTNGG-3′ and PESACB2 (reverse) 5′-GAAAACCATGGYTCNGCNAGYTGNCCN AGNAGYTG 3′ (*Nco*I sites are underlined and the substituted nucleotide in PAMOACB1 is shown in bold). Touch-down PCR was performed on total DNA of *P. fluorescens* ACB [26]. After initial denaturation for 5 min at 94 °C, the cycling program was as follows: 1 min 94 °C, 1 min 60 °C (2 °C decrease after every two cycles to 48 °C) and elongation at 72 °C for 2 min. In addition, 25 cycles were performed at a hybridization temperature of 48 °C and elongation for 1 min at 72 °C. The fragment obtained using the PESACB1 and PAPMO2 primers was ligated into the pCR2.1-TOPO vector and then transformed into *E. coli* TOP10F′ cells according to the recommendations of the manufacturer (Invitrogen). Plasmids containing insert were purified from overnight cultures with the High Pure™ plasmid isolation kit (Roche).

Preparation of a digoxigenin-labelled probe

To prepare the probe to screen the genomic library, the *hapD* gene in pCR2.1 was amplified with *Taq* polymerase (Roche) using the primers PESACBf (5′-GAAACCATG GCTCTTGACGTCGAGACGGCACAGCTG-3′) and PESACBr (5′-GAAAGGATCCTAAAAAGGGTTTCAGC CAAGGCTTGAT-3′) during 30 cycles of 1 min 94 °C, 1 min 60 °C and 1 min at 72 °C. The amplified fragment was isolated from gel and labelled with digoxigenin (DIG) by random-priming according to the method described by the DIG system user's guide for filter hybridization (Boehringer) yielding the DIG-labelled probe HAP2.

Screening of the genomic library

For screening, the constructed library was plated from the frozen stock on Luria–Bertani plates supplemented with 12.5 $\mu g \cdot mL^{-1}$ tetracycline and incubated overnight at 37 °C. Colonies were transferred to cellulose nitrate membranes. The membranes were processed and subsequently hybridized with the DIG-labelled HAP2 probe at 68 °C. Two primers, designed on the nondegenerated part of the *hapD* sequence were used to check *E. coli* clones which gave a positive signal after blotting: PESACB3 (5′-GAA GCCGTTCCATTTCT-3′) and PESACB4 (5′-GCCAAGG CTTGATCTGATC-3′). Cycling parameters were as follows: 1 min at 94 °C, 1 min at 57 °C and 1 min at 72 °C. As templates the pLAFR3 cosmids were isolated from the positive clones.

Cloning, expression and purification of recombinant HAPMO

The *hapE* gene was amplified with *Pwo* polymerase using the total DNA of *P. fluorescens* ACB as template. Therefore, two primers were designed: PAPMO1 (5′-CACGG CATATGAGCGCCTTCAATACC-3′, *Nde*I site underlined) and PAPMO2 (5′-CACGG*GGATCC*TCAACCTAGTTGG TAATCAGTCGG-3′, *Bam*HI site in italic type). Cycling parameters were as follows: 30 cycles of 1 min at 94 °C, 1 min at 56 °C and 1 min at 72 °C. After amplification, the gene was isolated from gel, digested with *Nde*I and *Bam*HI and ligated behind the T7 promoter of the *Nde*I/*Bam*HI digested expression vector pET-5a (Promega) yielding pHAPE1.

E. coli BL21(DE3)pLysS was transformed with this construct and grown in Luria–Bertani medium supplemented with 100 $\mu g \cdot mL^{-1}$ ampicillin and 35 $\mu g \cdot mL^{-1}$ chloramphenicol at 30 °C. When the D_{600} reached 0.8, 0.4 mM isopropyl thio-β-D-galactoside was added and the cells were grown for another 12–14 h at 20 °C. Cells (6 g) were harvested by centrifugation, resuspended in 50 mM potassium phosphate, pH 7.0, containing 0.1 mM EDTA and 0.1 mM dithiothreitol, and sonicated to prepare cell extract. After ultracentrifugation for 60 min at 110 000 ***g***, the supernatant was applied onto a ceramic hydroxyapatite column (2.5 × 12 cm), equilibrated with 50 mM potassium phosphate, pH 7.0, and eluted with the same buffer. Fractions containing HAPMO activity were pooled and loaded onto a Q-Sepharose column (2.5 × 18 cm) equilibrated with 50 mM potassium phosphate, pH 7.0. After washing with starting buffer, the enzyme was eluted with a

linear gradient of 0–1 M KCl in the same buffer. HAPMO eluted at a concentration of 0.6 M KCl. Active fractions were concentrated by ultrafiltration, dialysed in 50 mM potassium phosphate, pH 7.0, and stored at −80 °C.

PCR amplification to create truncated HAPMO variants

Two primers were designed to amplify truncated *hapE* genes. Primer PHAPMO3, 5′-CACGGCAT***ATG***GCCAGC GGCCGCGACTTCAAGGTGGTG-3′ annealed just upstream the part of the gene encoding the first Rossman fold sequence motif. Val136 was mutated to a methionine to create a *Nde*I site. Primer PHAPMO8, 5′-CACGGCAT ***ATG***GCCGAAGAAGCCGTGACCGCC-3′ was used to create a mutant lacking the part encoding the first 114 amino acids. Due to the introduction of a *Nde*I site, Ile115 was replaced by a methionine (*Nde*I sites underlined, start codon in bold, substituted codons in italic type). PCR with *Pwo* polymerase, using either PHAPMO3 or PHAPMO8 in combination with PAPMO2 as the reverse primer, under the same conditions as described for *hapE* amplification, yielded fragments which were cloned with *Nde*I/*Bam*HI in the pET5-a vector yielding pHAPE2 and pHAPE3, respectively. Successful cloning was confirmed by plasmid sequencing.

Site-directed mutagenesis

The Quickchange site-directed mutagenesis kit (Stratagene) was used to introduce a point mutation into HAPMO changing the glycine at position 490 into an alanine. Two primers were used, Primer 1 (5′-GTGTATGGCAC*GGC* GTTCCATGCCTCG-3′) and primer 2 (5′-CGAGGCATG GAA*GCC*GTGCCATACAC-3′). The mutagenic codon is shown in italic. The PCR reaction, with pHAPE1 as template, was performed under the conditions recommended by the manufacturer. Successful mutagenesis was confirmed by plasmid sequencing.

Steady-state kinetics

HAPMO activity was determined spectrophotometrically by monitoring the decrease of NADPH at 370 nm ($\varepsilon_{370} = 2.7$ mM^{-1}·cm^{-1}). Reaction mixtures (1 mL) typically contained 50 mM potassium phosphate pH 8.0, 0.25 mM NADPH and 50–100 nM enzyme. The reaction was started by the addition of 10 μL 0.1 M 4-hydroxyacetophenone in dimethylformamide. Specific activities were corrected for endogenous NADPH oxidase activity. One unit of HAPMO activity is defined as the amount of protein that oxidizes 1 μmol·min^{-1} NADPH. All kinetic measurements were performed at 30 °C using air-saturated buffers.

Steady-state kinetic parameters for acetophenone derivatives were estimated using a concentration range of 2.0 μM to 5.0 mM and a fixed concentration of 0.25 mM NADPH. The K'_m and V'_{max} for NADPH were estimated using a fixed concentration of 200 μM 4-hydroxyacetophenone and NADPH concentration range of 30–300 μM.

Formation of hydrogen peroxide was measured indirectly by adding a catalytic amount of catalase after completion of a HAPMO-catalysed conversion. Oxygen consumption and formation were monitored using an optical oxygen sensor 'Mops-1' (Prosense, Germany).

4-Hydroxyphenyl acetate hydrolase activity was determined spectrophotometrically by monitoring the production of *p*–nitrophenol at 405 nm ($\varepsilon_{405} = 7745$ M^{-1}·cm^{-1}, as determined experimentally at pH 7.0). Reaction mixtures contained 1–100 μg protein in 1 mL of a saturated solution of *p*-nitrophenyl acetate in phosphate buffer (pH 7.0).

Isotope labelling experiment

For ^{18}O incorporation experiments, 150 μL $H_2^{18}O$ was added to 327.5 μL 1.0 mM aromatic substrate in 50 mM phosphate buffer pH 7.0. After addition of HAPMO (2.5 μL, 200 μM) and NADPH (20 μL, 25 mM) the samples were incubated for 10 min and subsequently extracted with 1 mL diethylether. GC-MS analysis of the ether extracts was performed on a Hewlett Packard HP 5890 series II gas chromatograph and a Hewlett Packard HP 5971 mass spectrometer equipped with an HP-5 column. Samples (1 μL) were injected without derivatization, and the temperature program was 1 min isothermal at 80 °C followed by an increase to 150 °C at 10 °C·min^{-1} and finally 4 min at this temperature.

Analytical methods

Protein content was determined with Coomassie Brilliant Blue using BSA as the standard. SDS/PAGE was carried out on 12.5% slab gels. The Amersham Pharmacia Biotech low molecular mass calibration kit containing phosphorylase *b* (94 kDa), BSA (67 kDa), ovalbumin (43 kDa), carbonic anhydrase (30 kDa), soybean trypsin inhibitor (20.1 kDa), and α-lactalbumin (14.4 kDa) served as a reference. Proteins were stained with Coomassie Brilliant Blue G250. The relative molecular mass of native HAPMO was determined by FPLC gel filtration using a Superdex 200 HR 10/30 column (Pharmacia Biotech) running with 50 mM potassium phosphate buffer pH 7.0 containing 150 mM KCl. The column was calibrated with blue dextran 2000, thyroglobulin (669 kDa), ferritin (440 kDa), catalase (232 kDa), aldolase (158 kDa), lipoamide dehydrogenase (100 kDa), *p*-hydroxybenzoate hydroxylase (88 kDa), BSA (67 kDa), ovalbumin (43 kDa), chymotrypsinogen A (25 kDa), myoglobin (17.8 kDa) and cytochrome *c* (12.3 kDa).

The flavin prosthetic group of HAPMO was isolated and identified by reverse-phase HPLC according to the procedure described for 4-hydroxybenzoate 1-hydroxylase [27].

Absorption spectra were recorded at 25 °C on an Aminco DW-2000 spectrophotometer or a PerkinElmer Lambda Bio40 spectrophotometer. Flavin fluorescence emission spectra were recorded on an SPF-500 spectrofluorimeter essentially as described elsewhere [28].

DNA was cycle-sequenced with the Amersham Thermo Sequenase cycle-sequencing kit with 7-deaza-dGTP and Cy5 labelled fluorescent primers. Sequencing reaction mixtures were run on the Pharmacia ALF-Express DNA sequencer. The N-terminal amino-acid sequences of purified HAPMO and 4-hydroxyphenyl acetate hydrolase were determined by automatic Edman degradation at Eurosequence BV (Groningen, the Netherlands). The BLAST

program [29] at the National Center for Biotechnology Information (www.ncbi.nlm.nih.gov/BLAST/) was used to search for proteins showing sequence similarity. Multiple sequence alignments were made with the CLUSTAL W program at the European Bioinformatics Institute (www.ebi.ac.uk/clustalw) [30].

RESULTS

Purification of HAPMO from *P. fluorescens* ACB

Purification of HAPMO by anion exchange and hydrophobic chromatography resulted in a homogeneous enzyme preparation which is free of esterase activity. Table 1 summarizes a typical purification from 200 g 4-hydroxyacetophenone-grown *P. fluorescens* ACB cells. The enzyme was purified 25-fold with an overall yield of nearly 50%. SDS/PAGE revealed the presence of a single polypeptide chain, corresponding to an apparent molecular mass of $\approx$ 70 kDa. The purified enzyme elutes from an analytical Superdex 200 gel filtration column in one symmetrical peak with an apparent molecular mass of 140 $\pm$ 5 kDa. This suggests that native HAPMO from *P. fluorescens* ACB occurs as a homodimer in solution.

Spectral properties and identification of prosthetic group

The optical spectrum of HAPMO shows maxima at 382 and 440 nm, indicative of a flavoprotein (Fig. 1A). The ratio of the absorbance at 280 nm relative to that at 440 nm was 15.5. Unfolding of the enzyme revealed that the flavin cofactor is noncovalently bound. Incubation for 10 min of native HAPMO in the presence of 0.1% SDS leads to a final spectrum which corresponds to the absorbance of free FAD (Fig. 1A). The identity of the flavin prosthetic group was confirmed by HPLC and fluorescence analysis. From the absorbance difference between free and protein-bound FAD, a value of 12.4 $mM^{-1}\cdot cm^{-1}$ is estimated for the molar absorption coefficient (ε_{440}) of HAPMO at pH 7.0. Moreover, from the absorbance at 440 nm and protein content, it is concluded that each HAPMO subunit contains one molecule of FAD. The flavin fluorescence in HAPMO is strongly quenched. Comparison with flavin standards revealed that the relative fluorescence quantum yield of protein-bound FAD is less than 1% of free FAD (pH 7.0).

Catalytic properties

HAPMO from *P. fluorescens* ACB catalyses the FAD-dependent conversion of 4-hydroxyacetophenone to 4-hydroxyphenyl acetate with consumption of stoichiometric amounts of NADPH and molecular oxygen. Almost zero activity was found with NADH. The pH and temperature optima for enzyme catalysis are 7.5 and 30 °C, respectively. The specific activity of the purified enzyme is $\approx$ 5.5 μmol NADPH oxidized$\cdot min^{-1}\cdot mg^{-1}$ under the conditions of the standard assay (pH 8.0). Addition of free FAD to the assay mixture did not stimulate HAPMO activity, indicating that the flavin cofactor is tightly bound. To asses whether the FAD cofactor is involved in catalysis the enzyme was titrated with NADPH under anaerobic conditions. It was found that the flavin is readily reduced by NADPH (Fig. 1B). The full two-electron reduction of the FAD cofactor, as evidenced by the absorption decrease in the region 400–500 nm, indicates that all cofactor molecules participate in the reduction reaction. Upon restoring aerobic conditions by flushing the enzyme solution with air, the FAD cofactor is reoxidized within 5 min showing the ability of molecular oxygen to reoxidize the flavin cofactor. Oxygen consumption experiments performed in the absence or presence of catalase confirmed that in the absence of substrate the enzyme can act as an NADPH oxidase,

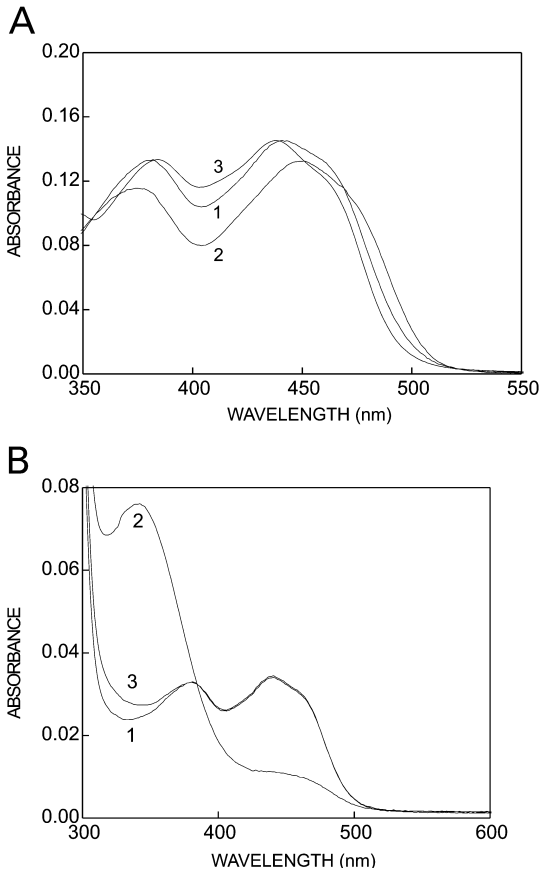

Fig. 1. Spectral properties of HAPMO from *P. fluorescens* ACB. The absorption spectra of HAPMO were recorded in 50 mM potassium phosphate buffer pH 7.0. (A) Absorption spectra of native (1) and unfolded HAPMO (2) and of the G490A mutant (3). HAPMO was unfolded by incubation of the enzyme in 0.1% SDS. (B) Spectral properties of oxidized and reduced HAPMO (3.0 μM).Oxidized HAPMO (1) was fully reduced by addition of 15 μM NADPH (2). Upon restoring aerobic conditions, the flavin becomes fully reoxidized (3).

Table 1. Purification of 4-hydroxyacetophenone monooxygenase from *P. fluorescens* ACB.

Step	Volume (mL)	Protein (mg)	Activity (U)	Specific activity ($U\cdot mg^{-1}$)	Yield (%)
Cell extract	800	30210	6552	0.22	100
Q-Sepharose	35	2610	4959	1.90	76
Phenyl-Sepharose	25	569	3129	5.50	48

Table 2. Steady-state kinetic parameters of HAPMO. All experiments were performed at 30 °C in air-saturated 50 mM potassium phosphate buffer pH 8.0. Apparent turnover rates (k'_{cat}) and apparent Michaelis constants (K'_m) were determined at fixed concentrations of either NADPH (250 μM) or 4-hydroxyacetophenone (200 μM).

Substrate	K'_m μM	k'_{cat} s^{-1}	k'_{cat}/K'_m $10^3\ s^{-1}\cdot M^{-1}$
NADPH	64 ± 14	9.3 ± 0.7	145
4-Hydroxyacetophenone	39 ± 9.0	10.1 ± 1.1	259
4-Aminoacetophenone	3.0 ± 1.0	12.3 ± 0.7	4100
4-Methylacetophenone	161 ± 36	6.3 ± 0.5	39
4-Methoxyacetophenone	541 ± 119	1.7 ± 0.2	3.1
4-Fluoroacetophenone	1040 ± 301	0.6 ± 0.1	0.6
acetophenone	2270 ± 873	4.5 ± 1.2	2.0
4-Hydroxy-3-methylacetophenone	380 ± 27	5.4 ± 0.1	14
4-Hydroxypropiophenone	12 ± 0.5	10.6 ± 0.4	883
4-Hydroxybenzaldehyde	101 ± 16	7.6 ± 0.3	75

forming hydrogen peroxide. Such an uncoupling reaction has also been observed for other flavin-dependent monooxygenases [6,31]. To determine the rate of the observed oxidase activity, consumption of NADPH was monitored in the absence of aromatic substrate revealing a low reactivity ($k'_{cat} = 0.11\cdot s^{-1}$, $K'_{m(NADPH)} = 5.0$ μM). Furthermore, analysis of the amount of hydrogen peroxide produced during conversion of 4-hydroxyacetophenone or acetophenone showed that in the presence of these aromatic substrates the uncoupling reaction does not occur as no hydrogen peroxide could be detected.

Substrate specificity

HAPMO catalyses the conversion of a wide range of acetophenone derivatives. The highest catalytic efficiency is observed with compounds bearing an electron donating substituent at the *para* position of the aromatic ring (Table 2). The apparent kinetic parameters listed in Table 2 indicate that the preference for these compounds is related not only to the rate of substrate conversion but also to substrate affinity. Table 2 also shows that the enzyme is rather active with the substrate analogues 4-hydroxybenzaldehyde and 4-hydroxypropiophenone. Cyclohexanone and cyclopentanone, which are substrates for some known Baeyer–Villiger monooxygenases [17], are not converted by HAPMO.

Isotope labelling experiments

To confirm the Baeyer–Villiger monooxygenation reaction and the formation of ester product, the enzymatic conversion was carried out with acetophenone and 4-hydroxyacetophenone as substrates in the presence of 30% (v/v) $H_2^{18}O$. After extraction of the reaction mixture with diethylether, samples were analysed by GC-MS. As a product from acetophenone conversion, phenyl acetate was identified giving a M^+ of *m*/*z* 136 and a base peak of *m*/*z* 94. The fragmentation pattern of the phenyl acetate spectrum was identical to that obtained after performing the enzymatic reaction with acetophenone in nonlabeled H_2O. This excludes the possibility that the oxygen atom inserted is derived from water and confirms the nature of the enzymatic Baeyer–Villiger monooxygenation reaction. Incubation with 4-hydroxyacetophenone showed only the formation of nonlabeled hydroquinone. This observation is attributed to the instability of the formed 4-hydroxyphenyl acetate.

Cloning strategy

During growth of *P. fluorescens* ACB on minimal medium with 4-hydroxyacetophenone as sole source of carbon and energy, it was observed that production of HAPMO coincided with an increase in esterase activity, causing hydrolysis of the formed 4-hydroxyphenyl acetate (data not shown). As both enzymes are metabolically coupled [13], it was expected that the corresponding genes might be located in one operon. Therefore, both enzymes were purified and the N-terminal amino-acid sequences were determined. For HAPMO, 20 residues were identified (Ser-Ala-Phe-Asn-Thr-Thr-Leu-Pro-Ser-Leu-Asp-Tyr-Asp-Asp-Asp-Thr-Leu-Arg-Glu-His) whereas for the esterase 21 residues (Thr-Leu-Asp-Val-Glu-Ser-Ala-Gln-Leu-Leu-Gly-Gln-Leu-Ala-Glu-Arg-Gly-Ala-Lys-Pro-Phe) were identified.

Four degenerated primers based on the N-terminal amino-acid sequences were designed; one forward primer and one reverse primer for each terminus. Touch-down PCR on total DNA of *P. fluorescens* ACB with the four logical primer combinations resulted in a fragment of 1035 bp, designated HAP1, when the primers PESACB1 and PAPMO2 were used. Taking the orientation of the primers into account it could be concluded that the esterase gene had been amplified. Analysis of the nucleotide sequence, after cloning HAP1 in the pCR2.1 TOPO vector, revealed an ORF of which the deduced amino-acid sequence showed high similarity with those of various lipases and esterases. Furthermore, the calculated molecular mass of ≈ 33 kDa and the N-terminal amino-acid residues confirmed that the ORF encoded the esterase. Downstream of the esterase gene, a partial ORF was identified that encodes a peptide fully consistent with the determined N-terminal peptide sequence of HAPMO. These findings prompted us to use the esterase gene, designated *hapD*, as a probe to screen a genomic library.

Genomic library screening and sequence of the *hapE* gene

A genomic library of *P. fluorescens* ACB was constructed using the cosmid vector pLAFR3 as described under Materials and methods. The *hapD* gene was amplified from pCR2.1, DIG-labelled and used as a probe. Screening of 1440 clones yielded two positive clones. PCR analysis confirmed that the *hapD* sequence was present on both plasmids and therefore the flanking regions of the esterase

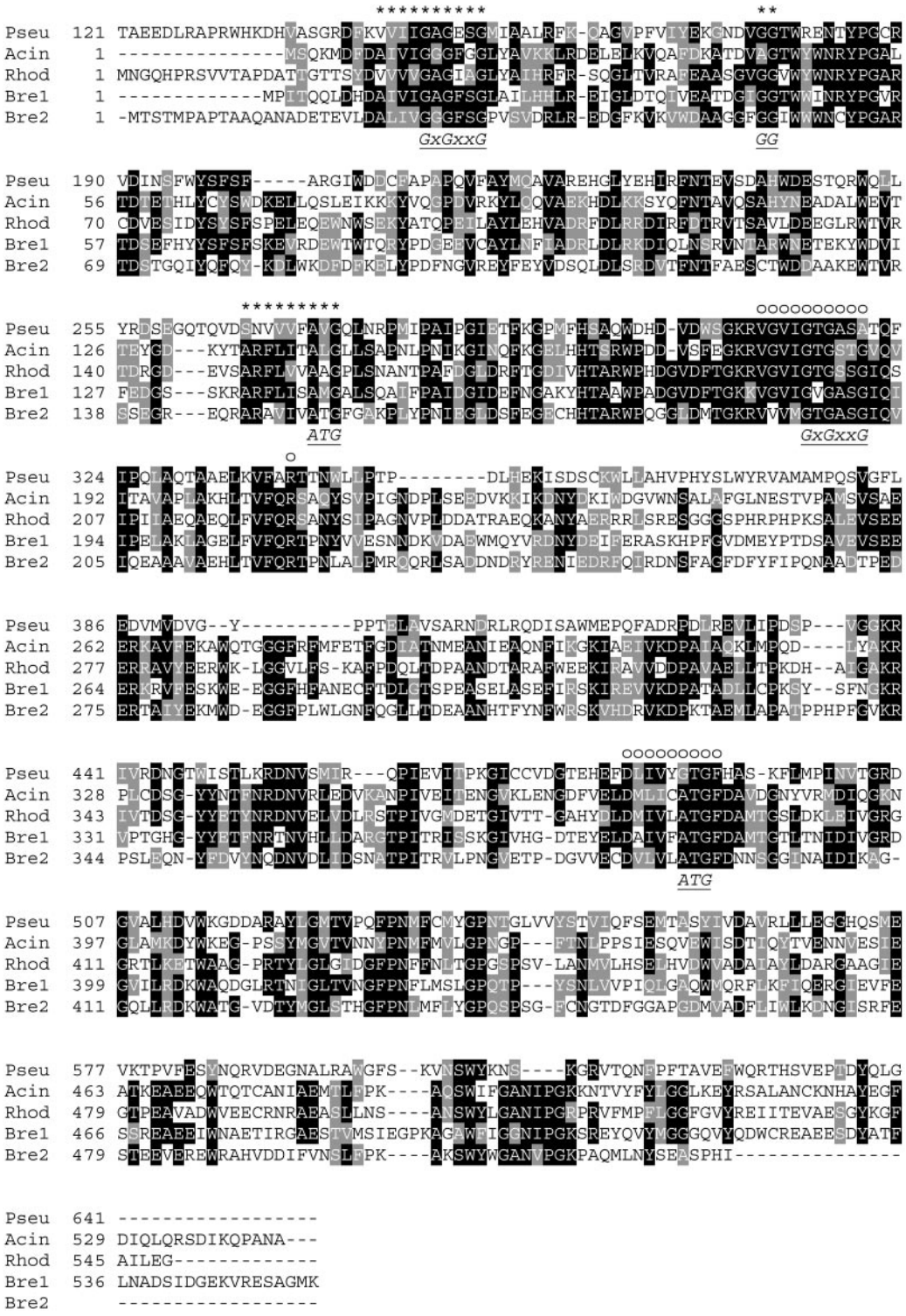

Fig. 2. Multiple sequence alignment of HAPMO from *P. fluorescens* ACB with other Baeyer–Villiger monooxygenases. The N-terminal truncated HAPMO sequence is aligned with cyclohexanone monooxygenase from *Acinetobacter* sp. NCIB 9871 (Acin, P12015) [41], steroid monooxygenase from *Rhodococcus rhodochrous* (Rhod, BAA24454) [40] and two cyclohexanone monooxygenases from a *Brevibacterium* isolate [42]. The regions indicative for FAD and NADPH binding are marked with asterisks and circles, respectively [34].

gene were sequenced. Sequencing of a 14-kb fragment revealed that the gene encoding HAPMO is the fifth ORF of an operon encoding genes involved in the degradation of 4-hydroxyacetophenone (data not shown). We therefore designated it *hapE*. The sequence has been deposited in the Genbank. The *hapE* gene encodes a protein of 640 amino acids with a deduced molecular mass of 71 884 Da, which is in line with the subunit molecular mass determined for the native enzyme.

Protein sequence comparison

Alignment with the known Baeyer–Villiger monooxygenases showed that HAPMO possesses 33 and 27% sequence identity with steroid monooxygenase from *Rhodococcus rhodochrous* and cyclohexanone monooxygenase from *Acinetobacter* sp. NCIB 9871, respectively. Sequence identities with the two newly identified cyclohexanone monooxygenases from a *Brevibacterium* isolate were 31% for Bre1 and 26% for Bre2 (Fig. 2). Intriguingly, HAPMO has an extension of ≈135 residues at the N-terminus which is not found in the other Baeyer–Villiger monooxygenase sequences. Furthermore, relatively high degrees of sequence identity were found for ORFs from *P. fluorescens* (38%), *Streptomyces coelicolor* (33%), *Mycobacterium tuberculosis* (33%), and a *Rhizobium* sp. (32%). This suggests that Baeyer–Villiger monooxygenases are widespread throughout the eubacteria. Lower degrees of sequence identity (20–25%) were found with the eukaryotic flavin-containing monooxygenases. The most conserved regions, located at the N-terminal half of the homologous sequences, contain two typical GXGXX(G/A) Rossman fold fingerprints (Fig. 2). These two sequence motifs are indicative of the presence of two βαβ dinucleotide binding folds [32] binding the adenylate parts of the FAD and NAD(P)H cofactors.

Expression and purification of recombinant HAPMO

For expression in *E. coli*, the *hapE* gene was placed under control of a T7 promoter in the expression vector pET5-a. When expression of HAPMO was induced in cells grown at 30 °C, part of the enzyme was produced as inclusion bodies as evidenced by SDS/PAGE analysis of whole cells. By lowering the temperature to 20 °C, formation of inclusion bodies could be prevented while yielding reasonable expression of soluble and active enzyme. Recombinant HAPMO was purified from *E. coli* BL21(DE3)pLysS harbouring pHAPE1 in a two-column procedure (Fig. 3). From 1-L culture, 30 mg enzyme could be purified with a yield of 70%. The A_{280}/A_{440} ratio of purified recombinant HAPMO was 15.6 which is similar to the value found for the enzyme isolated from *P. fluorescens* ACB. Moreover, the hydrodynamic properties and catalytic features of the recombinant enzyme are identical when compared to HAPMO purified from the wild-type strain.

Truncation of HAPMO

Because the N-terminal region of HAPMO does not show any similarity with known protein sequences it was anticipated that this part of the protein might not be essential for catalysis. To test this hypothesis, two mutant constructs, pHAPE2 and pHAPE3, were created that lack the coding region for the first 135 and 114 N-terminal amino-acid residues, respectively. However, SDS/PAGE analysis of cell extracts and whole cells transformed with these constructs showed that there was no visible expression of the truncated proteins at an induction temperature of 20 °C. Raising the induction temperature to 30 °C resulted in the formation of inclusion bodies. Activity was no detected in the cell extracts at either induction temperatures. Apparently, the N-terminal part of HAPMO is of importance for the structural integrity of the enzyme.

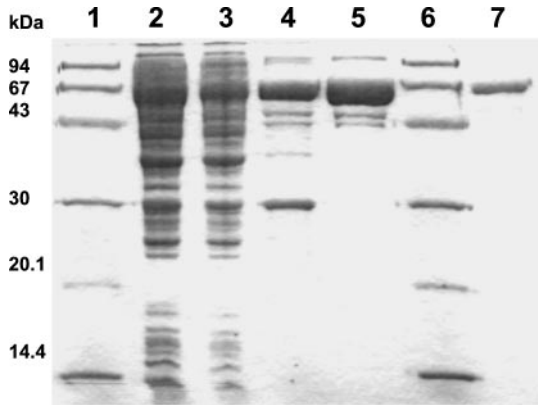

Fig. 3. SDS/PAGE of purification steps of recombinant 4-hydroxyacetophenone monooxygenase from *E. coli* BL21(DE3)pLysS. Lane 1 and 6, marker proteins; lane 2 and 3, cell extract at two concentrations; lane 4, hydroxyapatite fraction; lane 5 and 7, Q-Sepharose fraction at two concentrations.

Properties of the G490A mutant

Recently, an ATG sequence motif was described to be common for FAD and NAD(P)H binding proteins [33,34]. Since this sequence motif is also found in HAPMO (Fig. 2) and its function is still unclear, we decided to mutate the strictly conserved glycine 490 into an alanine. The mutant was overexpressed and purified according to the protocol for wild-type HAPMO. Gel filtration showed that the mutant enzyme was purified as a dimer. The ratio of the absorbance at 280 nm relative to that at 440 nm was 17.5, indicating that the enzyme is saturated with FAD. However, the shape of the flavin spectrum of the Gly490Ala mutant differs significantly from that of the wild-type enzyme (Fig. 1A). The oxidase activity of this mutant is significantly higher than that of the wild-type enzyme ($k'_{cat} = 0.4 \cdot s^{-1}$) but the Michaelis constant for NADPH is rather high ($K'_{m(NADPH)} = 700$ μM). In contrast with the wild-type enzyme, addition of 4-hydroxyacetophenone did not stimulate the rate of NADPH oxidation. However, GC-MS analysis revealed that the Gly490Ala mutant is still able to catalyse the Baeyer–Villiger oxidation of the aromatic substrate.

DISCUSSION

This paper describes the purification, characterization and cloning of HAPMO, a novel FAD-dependent Baeyer–Villiger

monooxygenase which is induced when *P. fluorescens* ACB is grown on 4-hydroxyacetophenone. HAPMO catalyses the first step in the degradation of 4-hydroxyacetophenone by inserting an oxygen atom in between the aromatic ring and the ketone side chain, yielding 4-hydroxyphenyl acetate. In addition to the conversion of 4-hydroxyacetophenone, HAPMO catalyses the oxygenation of a wide range of other aromatic ketones to the corresponding esters; by this, the enzyme is able to form a range of acylated phenols and catechols. As acylcatechols are valuable synthons for the fine chemical industry, HAPMO might develop as a useful biocatalytic tool. Furthermore, HAPMO resembles a recently isolated Baeyer–Villiger monooxygenase from *P. putida* JD1, that displays a similar substrate specificity and subunit molecular mass [16]. From this enzyme, only the N-terminal amino-acid sequence and two internal peptide sequences were determined which reveal a significant (80%) sequence identity with HAPMO. This indicates that Baeyer–Villiger monooxygenases acting on aromatic compounds frequently occur in nature.

Several Baeyer–Villiger monooxygenases acting on nonaromatic compounds have been identified in bacteria and fungi. All of these enzymes were shown to contain a flavin cofactor [35–39]. On the basis of the available biochemical data, Baeyer–Villiger monooxygenases have been divided into two subclasses [17]. Type I Baeyer–Villiger monooxygenases contain FAD as cofactor, are NADPH dependent and appear as monomers, homodimers or homotetramers. In contrast, type II Baeyer–Villiger monooxygenases contain FMN as cofactor, show NADH dependency and consist of two different subunits organized in a $\alpha_2\beta$ conformation. So far, only two type I Baeyer–Villiger monooxygenases have been cloned and characterized. These are steroid monooxygenase from *Rhodococcus rhodochrous* [40] and cyclohexanone monooxygenases from *Acinetobacter* NCIB 9871 [41] and a *Brevibacterium* isolate [42]. Within their N-termini, the Rossman fold fingerprint motif GxGxxG is found, which is thought to be involved in binding the ADP part of FAD [43].

HAPMO from *P. fluorescens* ACB is strictly dependent on NADPH and was found to be a homodimer with each 72-kDa subunit containing a noncovalently bound FAD. This and the significant sequence homology with cyclohexanone monooxygenase and steroid monooxygenase clearly classifies HAPMO as a type I Baeyer–Villiger monooxygenase. Besides the substrate specificity, there are some striking structural features that distinguishes HAPMO from the other type I Baeyer–Villiger monooxygenases. First, due to an N-terminal extension of $\approx$ 135 amino acids, the HAPMO subunit is much larger than that of related enzymes. As a consequence, the Rossman fold sequence motif indicative of FAD binding is not localized within the first 30 N-terminal amino-acid residues but is situated 148 residues from the N-terminus (Fig. 2). In cyclohexanone monooxygenase, this fingerprint sequence starts at residue 12 and in steroid monooxygenase at residue 27. We constructed truncated forms of HAPMO to explore the functionality of the N-terminal extension. However, the truncated HAPMO variants could not be expressed in a soluble form, suggesting that the N-terminal domain of HAPMO is important for the protein structural integrity. Another unique feature of HAPMO concerns the absence of a conserved aspartate near the N-terminal GxGxxG motif proposed to be typical for type I Baeyer–Villiger monooxygenases [17]. In the HAPMO sequence, a lysine (Lys143) is present at this position (Fig. 2). From the sequence analysis, we infer that this variance is probably not unique for type I Baeyer–Villiger monooxygenases as a similar feature is found in several of the HAPMO-related open reading frames.

Several sequence motifs have been described for proteins that bind both FAD and NADPH [5,34,44]. Besides the classical Rossman fold sequence motif (GXGXXG/A), a recently described ATG motif was shown to be indicative for FAD and NAD(P) binding domains [34]. Furthermore, two other short sequence motifs (GG and GD) have been identified to be indicative for a Rossman fold domain involved in FAD binding [34,44]. Upon alignment of the type I Baeyer–Villiger monooxygenase sequences, most of these sequence motifs could be identified displaying the following arrangement: GXGXXG–GG–ATG–GXGXXG–ATG (Fig. 2). In the HAPMO sequence, the only variations within these sequence motifs involve the first ATG motif (T→V) and the second GXGXXG motif (last G→A). The variation in the first ATG motif has also been observed in other flavoproteins whereas the alanine substitution in the second GXGXXG motif suggests that it is part of the NADPH binding domain [45,46]. This is in line with mutagenesis studies on a sequence-related flavin-containing monooxygenase from yeast where a conserved lysine near the second Rossman fold fingerprint was shown to be involved in binding of NADPH [47]. At this position a strictly conserved arginine is found in the known type I Baeyer–Villiger monooxygenase sequences (Arg339 in HAPMO, see Fig. 2) which, in analogy, probably interacts with the 2′-phosphate moiety of NADPH. The second ATG motif was recognized only recently. While Stehr *et al*. [33] have proposed a functional role of this hydrophobic sequence motif in substrate binding, analysis by Vallon [34] suggested a primary role in NADPH binding. We have assessed the functional role of this sequence motif by replacing the strictly conserved glycine residue. Analysis of the Gly490Ala mutant revealed a dramatic effect on binding and oxidation of NADPH. The NADPH oxidase activity was increased to some extent and the Michaelis constant for NADPH increased by two orders of magnitude. The mutant was still able to convert 4-hydroxyacetophenone indicating that Gly490 is not crucial for substrate recognition. Furthermore, spectral analysis indicated a perturbation of the flavin microenvironment. These results suggest that in HAPMO, the second ATG motif serves a structural function which is of importance for NADPH binding as proposed by Vallon [34].

The arrangement of sequence motifs in type I Baeyer–Villiger monooxygenases resembles the sequence organization of the pyridine nucleotide-dependent disulfide reductases [34] (e.g. glutathione reductase and lipoamide dehydrogenase) and the β subunit of glutamate synthase [46]. However, the Baeyer–Villiger monooxygenase sequences are lacking the GD motif involved in binding the FMN part of FAD [44]. The absence of this sequence motif or any other significant sequence similarity in the C-terminal half might well reflect the unique catalytic properties of Baeyer–Villiger monooxygenases and mechanistically related N-hydroxylating enzymes [19,48].

Expression of HAPMO, under the control of the T7 promotor [49], in *E. coli* BL21(DE3)pLysS resulted in relatively large amounts of soluble and active enzyme. This allows us to address in the near future the catalytic mechanism and structure–function relationship of this novel aromatic Baeyer–Villiger monooxygenase in further detail.

ACKNOWLEDGEMENTS

This work was supported by the Council for Chemical Sciences of the Netherlands Organization for Scientific Research (CW-NWO), division 'Procesvernieuwing voor een schoner milieu' and by the European Community (Framework IV, project BIO4-CT98-0267).

REFERENCES

1. Harayama, S., Kok, M. & Neidle, E.L. (1992) Functional and evolutionary relationships among diverse oxygenases. *Annu. Rev. Microbiol.* **46**, 565–601.
2. Suske, W.A., Held, M., Schmid, A., Fleischmann, T., Wubbolts, M.G. & Kohler, H.-P.E. (1997) Purification and characterization of 2-hydroxybiphenyl 3-monooxygenase, a novel NADH-dependent, FAD-containing aromatic hydroxylase from *Pseudomonas azelaica* HBP1. *J. Biol. Chem.* **272**, 24257–24265.
3. Arunachalam, U., Massey, V. & Miller, S.M. (1994) Mechanism of p-hydroxyphenylacetate-3-hydroxylase. A two-protein enzyme. *J. Biol. Chem.* **269**, 150–155.
4. Becker, D., Schrader, T. & Andreesen, J.R. (1997) Two-component flavin-dependent pyrrole-2-carboxylate monooxygenase from *Rhodococcus* sp. *Eur. J. Biochem.* **249**, 739–747.
5. Eppink, M.H.M., Schreuder, H.A. & van Berkel, W.J.H. (1997) Identification of a novel conserved sequence motif in flavoprotein hydroxylases with a putative dual function in FAD/NAD(P)H binding. *Protein Sci.* **6**, 2454–2458.
6. Entsch, B. & van Berkel, W.J.H. (1995) Structure and mechanism of para-hydroxybenzoate hydroxylase. *FASEB J.* **9**, 476–483.
7. Eppink, M.H.M., Overkamp, K.M., Schreuder, H.A. & Van Berkel, W.J.H. (1999) Switch of coenzyme specificity of *p*-hydroxybenzoate hydroxylase. *J. Mol. Biol.* **292**, 87–96.
8. Entsch, B., Ballou, D.P. & Massey, V. (1976) Flavin-oxygen derivatives involved in hydroxylation by *p*-hydroxybenzoate hydroxylase. *J. Biol. Chem.* **251**, 2550–2563.
9. Xun, L.Y. & Sandvik, E.R. (2000) Characterization of 4-hydroxyphenylacetate 3-hydroxylase (HpaB) of *Escherichia coli* as a reduced flavin adenine dinucleotide-utilizing monooxygenase. *Appl. Environ. Microbiol.* **66**, 481–486.
10. Galan, B., Diaz, E., Prieto, M.A. & Garcia, J.L. (2000) Functional analysis of the small component of the 4-hydroxyphenylacetate 3-monooxygenase of *Escherichia coli* W: a prototype of a new flavin: NAD(P)H reductase subfamily. *J. Bacteriol.* **182**, 627–636.
11. Cripps, R.E. (1975) The microbial metabolism of acetophenone. Metabolism of acetophenone and some chloroacetophenones by an *Arthrobacter* species. *Biochem. J.* **152**, 233–241.
12. Havel, J. & Reineke, W. (1993) Microbial degradation of chlorinated acetophenones. *Appl. Environ. Microbiol.* **59**, 2706–2712.
13. Higson, F.K. & Focht, D.D. (1990) Bacterial degradation of ring-chlorinated acetophenones. *Appl. Environ. Microbiol.* **56**, 3678–3685.
14. Darby, J.M., Taylor, D.G. & Hopper, D.J. (1987) Hydroquinone as the ring-fission substrate in the catabolism of 4-ethylphenol and 4-hydroxyacetophenone by *Pseudomonas putida* JD1. *J. Gen. Microbiol.* **133**, 2137–2146.
15. Jones, K.H., Trudgill, P.W. & Hopper, D.J. (1994) 4-Ethylphenol metabolism by *Aspergillus fumigatus*. *Appl. Environ. Microbiol.* **60**, 1978–1983.
16. Tanner, A. & Hopper, D.J. (2000) Conversion of 4-hydroxyacetophenone into 4-phenyl acetate by a flavin adenine dinucleotide-containing Baeyer–Villiger-type monooxygenase. *J. Bacteriol.* **182**, 6565–6569.
17. Willetts, A. (1997) Structural studies and synthetic applications of Baeyer-Villiger monooxygenases. *Trends Biotechnol.* **15**, 55–62.
18. Ryerson, C.C., Ballou, D.P. & Walsh, C. (1982) Mechanistic studies on cyclohexanone oxygenase. *Biochemistry* **21**, 2644–2655.
19. Sheng, D., Ballou, D.P. & Massey, V. (1999) The intermediates involved in the catalytic reaction of cyclohexanone monooxygenase. In *Flavins and Flavoproteins, 13th International Congress on Flavins and Flavoproteins* (Ghisla, S., Kroneck, P., Macheroux, P. & Sund, H., eds), pp. 367–370. Agency for Scientific Publication, Berlin.
20. Massey, V. (1994) Activation of molecular oxygen by flavins and flavoproteins. *J. Biol. Chem.* **269**, 22459–22462.
21. Moonen, M.J.H., Rietjens, I.M.C.M. & van Berkel, W.J.H. (1999) Purification and some properties of acetophenone monooxygenase. In *Flavins and Flavoproteins, 13th International Congress on Flavins and Flavoproteins* (Ghisla, S., Kroneck, P., Macheroux, P. & Sund, H., eds), pp. 375–378. Agency for Scientific Publication, Berlin.
22. Krockel, L. & Focht, D.D. (1987) Construction of chlorobenzene-utilizing recombinants by progenitive manifestation of a rare event. *Appl. Environ. Microbiol.* **53**, 2470–2475.
23. Sambrook, J., Fritsch, E.F. & Maniatis, T. (1989) *Molecular Cloning: A Laboratory Manual*, 2nd edn. Cold Spring Harbor Laboratory Press, New York.
24. Staskawicz, B., Dahlbeck, D., Keen, N. & Napoli, C. (1987) Molecular characterization of cloned avirulence genes from race 0 and race 1 of *Pseudomonas syringae* pv. *glycinea*. *J. Bacteriol.* **169**, 5789–5794.
25. Innis, M.A. & Gelfand, D.H. (1990) A guide to methods and amplification. In *PCR Protocols* (Innis, M.A., Gelfand, D.H., Sninsky, J.J. & White, T.J., eds), pp. 3–12. Academic Press, San Diego.
26. Don, R.H., Cox, P.T., Wainwright, B.J., Baker, K. & Mattick, J.S. (1991) 'Touchdown' PCR to circumvent spurious priming during gene amplification. *Nucleic Acids Res.* **19**, 4008.
27. Eppink, M.H.M., Boeren, S.A., Vervoort, J. & van Berkel, W.J.H. (1997) Purification and properties of 4-hydroxybenzoate 1-hydroxylase (decarboxylating), a novel flavin adenine dinucleotide-dependent monooxygenase from *Candida parapsilosis* CBS604. *J. Bacteriol.* **179**, 6680–6687.
28. Eschrich, K., van der Bolt, F.J.T., de Kok, A. & van Berkel, W.J.H. (1993) Role of Tyr201 and Tyr385 in substrate activation by *p*-hydroxybenzoate hydroxylase from *Pseudomonas fluorescens*. *Eur. J. Biochem.* **216**, 137–146.
29. Altschul, S.F., Madden, T.L., Schaeffer, A.A., Zhang, J., Zhang, Z., Miller, W. & Lipman, D.J. (1997) Gapped BLAST and PSI-BLAST: a new generation of protein database search programs. *Nucleic Acids Res.* **25**, 3389–3402.
30. Thompson, J.D., Higgins, D.G. & Gibson, T.J. (1994) CLUSTAL W: improving the sensitivity of progressive multiple sequence alignment through sequence weighting, position-specific gap penalties and weight matrix choice. *Nucleic Acids Res.* **22**, 4673–4680.
31. Suske, W.A., van Berkel, W.J.H. & Kohler, H.P.E. (1999) Catalytic mechanism of 2-hydroxybiphenyl 3-monooxygenase, a flavoprotein from *Pseudomonas azelaica* HBP1. *J. Biol. Chem.* **274**, 33355–33365.
32. Wierenga, R.K., Terpstra, P. & Hol, W.G. (1986) Prediction of the occurrence of the ADP-binding beta alpha beta-fold in proteins,

using an amino-acid sequence fingerprint. *J. Mol. Biol.* **187**, 101–107.

33. Stehr, M., Diekmann, H., Smau, L., Seth, O., Ghisla, S., Singh, M. & Macheroux, P. (1998) A hydrophobic sequence motif common to N-hydroxylating enzymes. *Trends Biochem. Sci.* **23**, 56–57.
34. Vallon, O. (2000) New sequence motifs in flavoproteins: Evidence for common ancestry and tools to predict structure. *Proteins* **38**, 95–114.
35. Donoghue, N.A., Norris, D.B. & Trudgill, P.W. (1976) The purification and properties of cyclohexanone oxygenase from *Nocardia globerula* CL1 and *Acinetobacter* NCIB 9871. *Eur. J. Biochem.* **63**, 175–192.
36. Itagaki, E. (1986) Studies on steroid monooxygenase from *Cylindrocarpon radicicola* ATCC 11011. Purification and characterization. *J. Biochem.* **99**, 815–824.
37. Miyamoto, M., Matsumoto, J., Iwaya, T. & Itagaki, E. (1995) Bacterial steroid monooxygenase catalyzing the Baeyer–Villiger oxidation of C21-ketosteroids from *Rhodococcus rhodochrous*: the isolation and characterization. *Biochim. Biophys. Acta* **1251**, 115–124.
38. Ougham, H.J., Taylor, D.G. & Trudgill, P.W. (1983) Camphor revisited: involvement of a unique monooxygenase in metabolism of 2-oxo-delta 3-4,5,5-trimethylcyclopentenylacetic acid by *Pseudomonas putida*. *J. Bacteriol.* **153**, 140–152.
39. van der Werf, M.J. (2000) Purification and characterization of a Baeyer-Villiger mono-oxygenase from *Rhodococcus erythropolis* DCL14 involved in three different monocyclic monoterpene degradation pathways. *Biochem. J.* **3**, 693–701.
40. Morii, S., Sawamoto, S., Yamauchi, Y., Miyamoto, M., Iwami, M. & Itagaki, E. (1999) Steroid monooxygenase of *Rhodococcus rhodochrous*: Sequencing of the genomic DNA, and hyperexpression, purification, and characterization of the recombinant enzyme. *J. Biochem.* **126**, 624–631.
41. Chen, Y.C., Peoples, O.P. & Walsh, C.T. (1988) *Acinetobacter* cyclohexanone monooxygenase: gene cloning and sequence determination. *J. Bacteriol.* **170**, 781–789.
42. Brzostowicz, P.C., Gibson, K.L., Thomas, S.M., Blasko, M.S. & Rouviere, P.E. (2000) Simultaneous identification of two cyclohexanone oxidation genes from an environmental *Brevibacterium* isolate using mRNA differential display. *J. Bacteriol.* **182**, 4241–4248.
43. Wierenga, R.K., Drenth, J. & Schulz, G.E. (1983) Comparison of the three-dimensional protein and nucleotide structure of the FAD-binding domain of *p*-hydroxybenzoate hydroxylase with the FAD- as well as NADPH-binding domains of glutathione reductase. *J. Mol. Biol.* **167**, 725–739.
44. Eggink, G., Engel, H., Vriend, G., Terpstra, P. & Witholt, B. (1990) Rubredoxin reductase of *Pseudomonas oleovorans*. Structural relationship to other flavoprotein oxidoreductases based on one NAD and two FAD fingerprints. *J. Mol. Biol.* **212**, 135–142.
45. Bork, P. & Grunwald, C. (1990) Recognition of different nucleotide-binding sites in primary structures using a property-pattern approach. *Eur. J. Biochem.* **191**, 347–358.
46. Morandi, P., Valzasina, B., Colombo, C., Curti, B. & Vanoni, M.A. (2000) Glutamate synthase: identification of the NADPH-binding site by site-directed mutagenesis. *Biochemistry* **39**, 727–735.
47. Suh, J.K., Poulsen, L.L., Ziegler, D.M. & Robertus, J.D. (1999) Lysine 219 participates in NADPH specificity in a flavin-containing monooxygenase from *Saccharomyces cerevisiae*. *Arch. Biochem. Biophys.* **372**, 360–366.
48. van Berkel, W.J.H., Eppink, M.H.M. & Schreuder, H.A. (1999) Coenzyme recognition by flavoprotein aromatic hydroxylases. In *Flavins and Flavoproteins, 13th International Congress on Flavins and Flavoproteins* (Ghisla, S., Kroneck, P., Macheroux, P. & Sund, H., eds), pp. 343–349. Agency for Scientific Publication, Berlin.
49. Studier, F.W. & Moffatt, B.A. (1986) Use of bacteriophage T7 RNA polymerase to direct selective high-level expression of cloned genes. *J. Mol. Biol.* **189**, 113–130.